7TH INTERNATIONAL CONFERENCE

ON

CONTACT MECHANICS AND WEAR OF RAIL/WHEEL SYSTEMS

www.materialsaustralia.com.au/cm2006/

24th – 27th September 2006
Brisbane
AUSTRALIA

PROCEEDINGS
Volume Two

Revision 1

ISBN 1 876855 27 4

7th International Conference on Contact Mechanics and Wear of Rail/Wheel Systems (CM2006), Brisbane, Australia, September 24-26, 2006

FRACTURE MECHANICAL ANALYSIS AND ASSESSMENT OF THE EXTENSION OF ROLLING CONTACT FATIGUE CRACKS IN RAILWAY RAILS

Dr.-Ing. Thomas Schnitzer[*], Prof. Dr.-Ing. habil. Karl-Otto Edel[#]

[*#]Fachhochschule Brandenburg – University of Applied Sciences, Germany

[*]th.schnitzer@gmx.de
[#]edel@fh-brandenburg.de

ABSTRACT

Rolling contact fatigue generates cracks on the running surface of high strength railway rails which grow under a small angle into the rail head. These cracks can cause in its last stage the fracturing of the rail. The crack extension behaviour is – as the origin of these cracks too – influenced by the cold working of the rail steel. The crack growth in the first stage is fracture mechanically analyzed by means of two-dimensional modelling. The simulation results are assessed for the use of rail grinding. A criterion for the change of the crack growth direction could not be derived, but the following stages of the crack growth in the transverse direction and the final fracture and the conditions for secondary fractures are considered.

1 THE OCCURRENCE OF RAIL DEFECTS

By means of many technical developments the operation of the railway especially the properties of the railway rails have been improved. According to the increased standards the resistance of the rails are increased. The increased strength properties lead to an increased wear resistance of the rails. Due to the minimized wear of the high strength rails the initial defects were not removed by the service itself. The initial defects develop into rolling contact fatigue cracks.

2 ROLLING CONTACT FATIGUE (RCF) AND THE CONSEQUENCES

The RCF defects are classified according to their geometry as either squats or head checks. Squats are cracklike single defects in the middle area of the running surface which originate on the surface and extend under a shallow angle in the direction of the train, in a smaller amount in the opposite direction. Head checks are cracklike defects on the running edge in a large number which are shallowly inclined in the driving direction. Both kinds of defects originate from the cold working of the rail steel due to the contact load.

The fine Head Checks have a distance from 1 to 7mm from each other. This type of the crack formation mainly appears in bendy track sections which are exposed to a high traffic load [1]. While the consequences of the Head Checks were noticed for a long time only with regard to spalling at the running edge, it has been known for several decades [2] that these defects also can cause the fracture of the rail. The danger of a derailment by fractures because of Head Checks has to be assessed similarly as the endangering by cracks which starts on engine burn defects at the running surface over longer rail areas [3]. Since the Head Checks extend over large areas of the rail large rail pieces can break off in the end.

Since it was known that RCF not only causes cracks but also fractures, the usual rail grinding was used as countermeasure for the crack extension. In addition the expert committee 19 of the European Rail Research Institute (ERRI) dealt with the difficulties of these defects in the nineties.

The derailment of a high speed train of the GNER at October, 17 in 2000 at Hatfield near London shows the serious consequences of failure of RCF damaged rails. In a curved track the train destroyed at a speed of 115mph the outer rail of 35m length in more then 200 pieces. Four passengers died at this accident. [4]

3 FEM CALCULATION OF STRESS INTENSITY FACTORS OF RCF CRACKS [5, 6]

To reduce the variety of influence parameters the fracture mechanical problem was solved by means of a two dimensional model of contact and bending (fig. 1). Because of the idealisation as a two-dimensional model the combined contact-bending-load could not be simply realized with a wheel force. Therefore the dynamic wheel force was used first to realize the true bending of the rail. Then the rail was held tight in this bent situation and the wheel force was 20% increased to realize the true contact force on the running surface, which was found out by a comparison calculation.

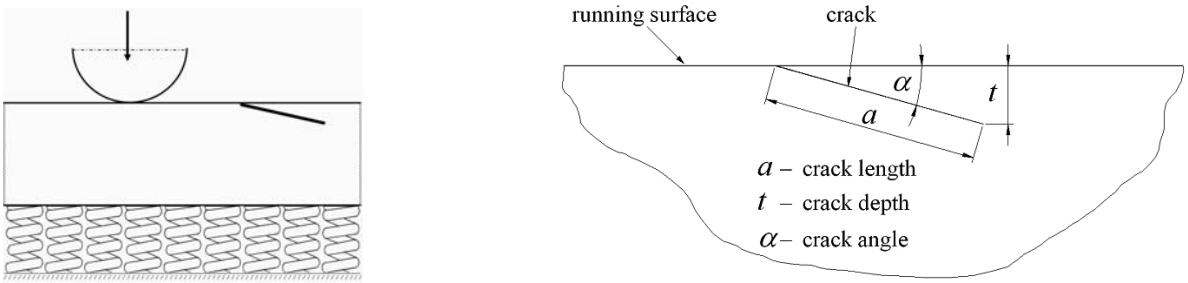

Figure 1. Fracture mechanical model, definition of length, depth and angle of the RCF cracks

The variation of the distance between the wheel and the crack shows that the essential crack tip loading is given by the stress intensity factor K_{II} (fig. 2).

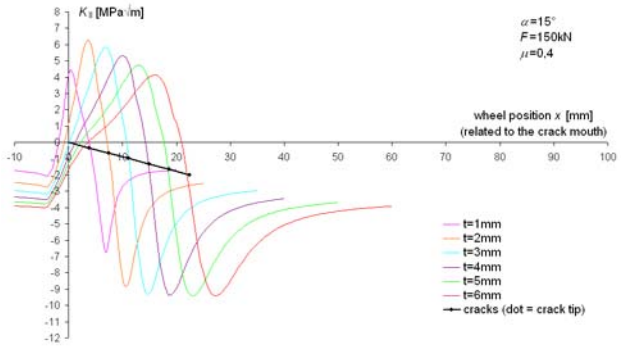

Figure 2. The contact-bending-load caused K_{II} vs. wheel position related to the crack mouth

The single crack shows the highest tip loading in comparison with the multiple cracks of equal, smaller respective larger crack size. Therefore the single crack was generally adopted for all following analyses. Figure 3 shows the range ΔK_{II} of the stress intensity factor of Mode II for different crack front depths t and crack angles α.

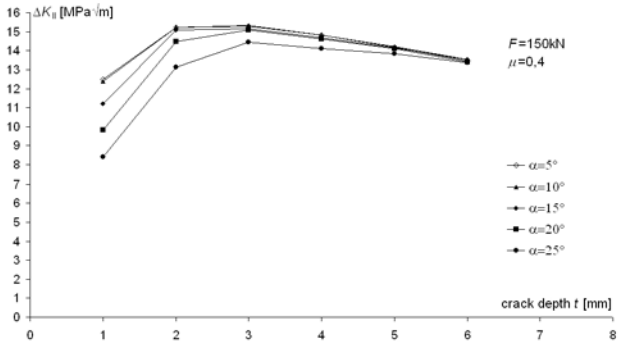

Figure 3. The contact-bending-load caused ΔK_{II} vs. crack depth

4 MATERIAL INVESTIGATION ON COLD WORKED RAIL STEEL [5, 6]

Used rails show a considerable enlargement of the hardness on the gauge side of the rail head with modified fracture mechanical properties. Since no fracture mechanical specimens with the relevant properties of the cold worked steel can be taken from the running edge area, specimens with a thickness of 37.5mm taken from the rail head were cold worked down in different measure to thicknesses of at least 25mm. From this preconditioned material DCT-specimens for the determination of the crack growth properties were taken. The investigation of the growing cracks shows a pronounced orthotropy of the crack growing properties [7, 8].

The tests were carried out with specimens in whom the direction of the cold working direction and the direction of the notch have differences of 15° and 30°. Despite the original Mode I loading of the notches, the cracks extend nearly straight in the direction of the cold working (fig. 4).

Figure 4. Specimen with 30° deviation between the direction of cold working and of the notch

The evaluation of the crack growing tests was carried out in analogy to the calculation of the energy release rate (or crack extension force) G by means of the relation

$$\Delta K_V = \sqrt{\Delta K_I^2 + \Delta K_{II}^2}$$

for the threshold value $\Delta K_{V,th}$ and for the growing properties by means of the modified Paris law

$$\frac{da}{dN} = C \cdot \Delta K_V^n = C \cdot \sqrt{\Delta K_I^2 + \Delta K_{II}^2}^n .$$

All specimens were evaluated individually by means of the FEM according to the experimental determined crack parameters.

5 SIMULATION OF THE BEHAVIOUR OF THE RCF CRACKS [5, 6]

The material investigations show a dependence of the fracture mechanical properties on the degree of cold working of the rail steel. The different material properties are correlated by means of the hardness HV30 to a certain depth under the surface of the rail head. The change of the hardness in the rail is given in fig. 5. The crack growth properties are compiled in table 1 depending on

the degree of cold working respective on the depth under the surface. Between the values (n, log C) it was interpolated linearly, up to the "crack depth" $t = 0$ mm it was extrapolated linearly.

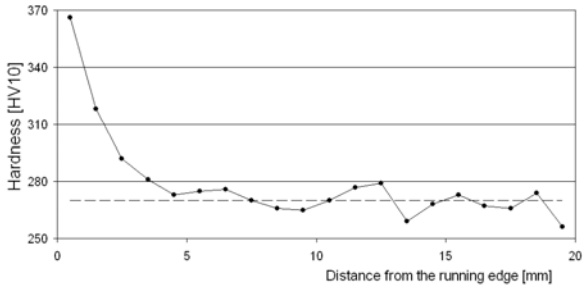

Figure .: Change of the Hardness HV10 from the running edge into the inside of the rail damaged by Head Checks

Table 1. Crack growth properties depending on the crack depth t

Degree of cold working	hardness HV30	Crack depth t in mm	Paris exponent n	log. Parisfaktor log C	Paris factor C in $\mathrm{mm}\cdot(\mathrm{N/mm^{3/2}})^{-n}$	Standard deviation $\tilde{s}_{\ln da/dN}$	
extrapolated		0,00	1,902	-9,12952	$7{,}4214 \cdot 10^{-10}$		mean value: 0,2590
33,1%	320	1,45	2,252	-10,37022	$4{,}2636 \cdot 10^{-11}$	0,26704	
20,5%	301	2,15	2,419	-10,96194	$1{,}0916 \cdot 10^{-11}$	0,19276	
10,7%	287	2,95	2,933	-12,40079	$3{,}9738 \cdot 10^{-13}$	0,29264	
0%	273	5,00	5,477	-19,70270	$1{,}9829 \cdot 10^{-20}$	0,28354	

The scattering crack growth was considered by the equation

$$\left.\frac{\mathrm{d}a}{\mathrm{d}N}\right|_{\text{scattering}} = \frac{\mathrm{d}a}{\mathrm{d}N}(P) = C \cdot \exp(z_{\mathrm{n}} \cdot \tilde{s}_{\ln\, \mathrm{d}a/\mathrm{d}N}) \cdot \Delta K_{\mathrm{V}}^{n}$$

with z_{n} as a normal distributed random figure with the mean 0 and the standard deviation 1.

In a preliminary analysis the non-exceeding crack sizes t_{th} were calculates for the different crack angles. The initial crack size for the following crack growing calculation according to the modified Paris law was assumed as $t = 0.5$ mm .

The results of the FE calculations with the two-dimensional model shown in fig. 3 are the basis for the load assumptions at the simulation calculations. It was interpolated linearly between the calculated values ΔK_{II} for the crack depths of 1, 2, 3, 4, 5 and 6 mm. For the "crack depth" of 0 mm it was assumed that $\Delta K_{\mathrm{II}} = 0$.

The crack growth calculations between a predefined initial crack size and a predefined final crack size can be varied so that the initial crack size is assumed as constant or that the final crack size is assumed as constant. The latter variant is for the practice of greater importance because the cracks of different size shall not exceed a limit dimension. The results represented in fig. 6 show a very broad scatter field. The curve which has a crack growth rate probability of 90% is representative for the fastest crack growth.

The RCF cracks existing in railway rails have different angles relating to the running surface. In the Monte Carlo simulation were used: Head Checks – mean 16,4°, standard deviation 4,2° (according to 47 own measurements), Squats – mean 10,1°, standard deviation 3,6° (according to 49 measurements [9]).

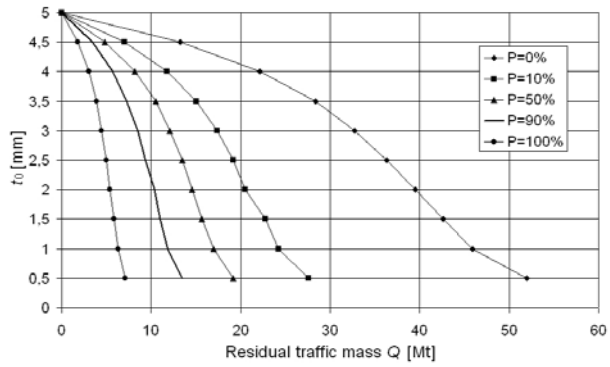

Figure 6. Residual traffic mass for a 15° inclined crack at a crack growth from t_0 up to a permitted crack depth $t_{allowable}$ = 5mm

That curves which represent the fastest crack growth are given in figure 7.

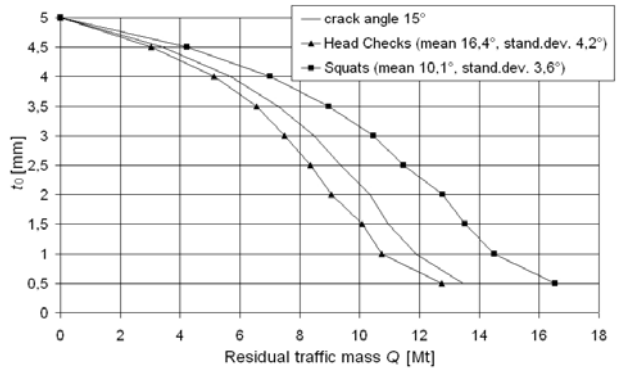

Figure 7. Residual traffic mass for the 90%-crack-growth from t_0 up to a permitted crack depth $t_{allowable}$= 5mm for 15° inclined cracks as well as for Head Checks and Squats

As experience shows the inclined RCF cracks change there growing direction into the cross section of the rail in the depth of about 5mm. A theoretical criterion or criterion found out experimentally for the change of direction could not be found. Therefore this crack depth must be considered as the operating limit dimension $t_{\text{allowable,max}}$.

The representative crack growth curves which are found out by Monte Carlo simulation are surpassed in 10% of the cases, the permitted crack growth curves (with maximum crack growth speed) must be derived from them by safety coefficients chosen usefully. These assessments were realized by two different considerations and are illustrated in fig. 8.

Variant 1: The representative curve is moved to below:

$$t_{\text{allowable}} = t_{\text{allowable,max}} - \Delta t_{\max} \text{ with}$$

$$\Delta t_{\max} = S_{\dot{a}} \cdot \Delta t(P_{\dot{a}} = 90\%) \text{ and } S_{\dot{a}} \geq \frac{\Delta t_{\max}}{\Delta t(P_{\dot{a}} = 90\%)} \approx 1.5$$

Variant 2: The representative curve is moved to the left:

$$N_{\text{NDT-Cycle}} = N_{\text{allowable}} = \frac{N(P_{\dot{a}} = 90\%)}{S_{\mathrm{d}a/\mathrm{d}N}} \text{ with } S_{\mathrm{d}a/\mathrm{d}N} = S_{\sigma}^{n},$$

$S_{\sigma} = 1.2$, Paris exponent $n \approx 2$

The assessment by variant 2 shows the more conservative results. The assessment by variant 1 should not correspondingly be exceeded in the practice.

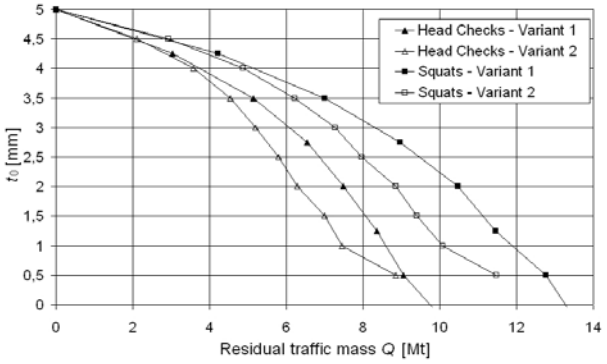

Figure 8. Assessment diagram for RCF defects in rails UIC60

There are no practical experiences with growing RCF cracks. Therefore it is useful to replace rails with cracks of certain depth found non-destructively at the latest in accordance with the representative crack growth curve (variant 1 or 2). If there exist sufficient practical experiences at a later time, then the next non-destructive rail test could be carried out within the permitted rest operating time.

Regarding the specification of the rail grinding cycle the phase of the crack initiation could not be included in the fracture mechanical analyses and assessments. For this reason a periodical non-destructive test with determination of the damage depth is required. If a certain depth of the crack fronts has been established, the remaining time for the execution of the rail grinding process can be fixed with the help of the assessment diagrams. Practical experiences with a railway line show that the crack initiation phase is about three years. After this time 0.54mm deep cracks had formed [10].

6 SIMULATION OF THE BEHAVIOUR OF THE TRANSVERSAL CRACKS [5]

The analysis of the stable and the unstable extension of transverse cracks in rails UIC60 with a horizontal crack front (fig. 9) was carried out using the extreme value of the so called negative bending moment between the both action points of the wheel forces of the size

$$M_{\mathrm{b}} = 2 \cdot \frac{F_{\text{Wheel}} \cdot L}{4} \cdot \exp(-\pi / 2)$$

with the dynamical wheel force of $F_{\text{Wheel}} = 150\text{kN}$ and the basic length $L = 651\text{mm}$. The temperature stresses are given by the difference between the real rail temperature and the stress free temperature. It was assumed that the original stress free temperature was equal distributed between 20°C and 26°C. The real stress free temperature scatters with a standard deviation of 4,2K around the original value.

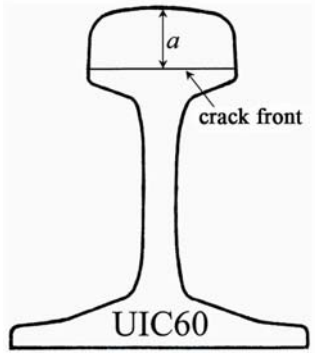

Figure 9. Fracture mechanical model of transverse cracks

The fracture condition $K_{\text{I}\max} = K_{\text{Ic}}$ is a non-linear equation for the crack size *a*. For the simulated fracture conditions these relation shows a considerable scatter (fig. 10).

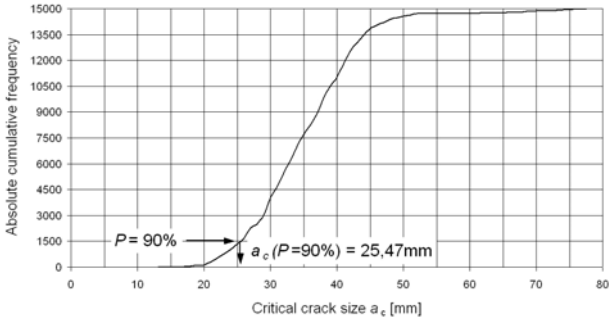

Figure 10. Probability distribution of the size of critical transverse cracks in rails UIC60 derived by Monte Carlo simulation

To exclude the rail failure, the maximum allowable crack size which lay under the real minimum of the critical crack size must be prescribed. Starting from the representative minimum value of the critical crack size (with a survival probability of 90%) and a safety factor of 1.4 which is related to the crack size [11] it follows

$$a_{\text{allowable,max}} = \frac{a_{\text{c}}(P_{\text{survival}} = 90\%)}{S_{ac}} = \frac{25.47\text{mm}}{1.4} \approx 18\text{mm}\,.$$

The growth of the transverse crack in rails UIC60 leads for the given wheel forces and temperatures to widely scattered results (fig. 11). The curve of the allowed, i.e. fastest crack growth is derived by the relation [11]

$$a_{\text{allowable}} = a_{\text{allowable,max}} - \Delta a_{\max} \text{ with}$$
$$\Delta a_{\max} = S_{\dot{a}} \cdot \Delta a(P_{\dot{a}} = 90\%) \text{ and}$$
$$S_{\dot{a}} \geq \frac{\Delta a_{\max}}{\Delta a(P_{\dot{a}} = 90\%)} \approx 1.5\,.$$

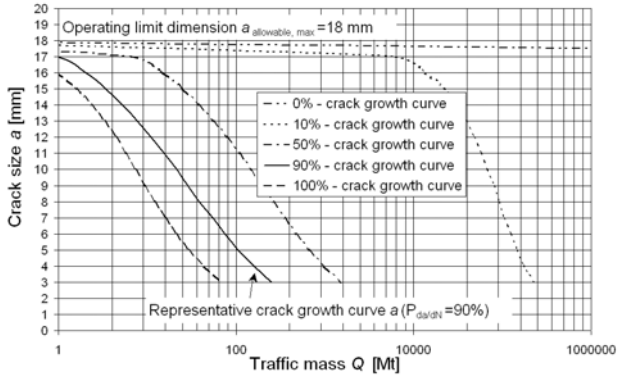

Figure 11. The scatter field of growth curves of transverse cracks in the head of rails UIC60

Depending on the track loading conditions the residual life can enclose different temperature periods. If necessary it can consider the rail temperature distribution of the whole year or the temperature distribution of the of the winter quarter (fig. 12).

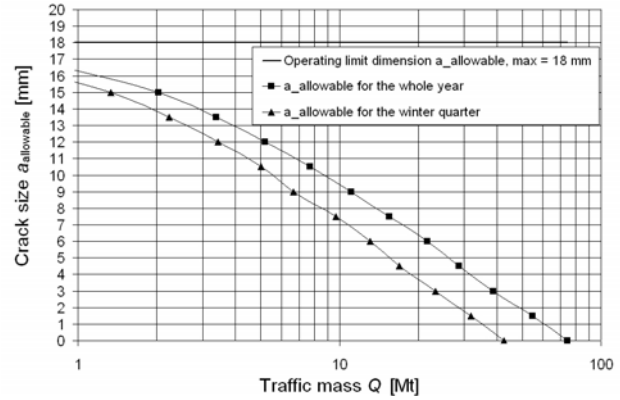

Figure 12. Assessment diagram for RCF caused transverse cracks in the head of rails UIC60 considering the temperature loading in the whole year resp. the winter quarter

7 SIMULATION OF FOLLOWING FAILURES [5]

A rail with a transversal fracture caused by RCF cracks, which is used further, is loaded by bending like a beam fixed on one side (with a length of maximum about 450mm). Japanese examinations [12] show in this case with 250km/h vehicle speed that the wheel forces increase from their static value (100kN) to the double value at a standard deviation of the speed coefficient of 0.31.

Under the assumption of transverse cracks with a horizontal crack front it results in a representative minimum value of the critical crack size

$$a_{\text{c}}(P_{\text{survival}} = 90\%) = 5.22\text{mm}$$

The reduction of the stress intensity factors to 66% - to take the bend of the crack front on the one hand and the residual compression stresses at the running surface on the other hand into consideration - results in a critical crack size $a_{\text{c}}(P_{\text{survival}} = 90\%) = 9.32\text{mm}$. Under these almost realistic conditions the minimum value of the size of critical cracks can lie within the range of 6 to 7mm and with that in the size of the deepest RCF cracks. If there are such deep RCF cracks it is not excluded, that crack damaged rails will break into many small pieces in a kind of chain reaction - as it was the case in Hatfield.

8 CONCLUSIONS

The problem of crack extension due to RCF which is important for all railway rails is considered by means of the linear fracture mechanics. The essential assumptions are:

- The cold working of the rail steel is essential for crack growth.
- The modelling as a two-dimensional problem is at present stage better than a complete three-dimensional FEM analysis to get a practically applicable solution.
- The rail is loaded on its running surface with distinct forces to realize the bending (with compression stresses in the head) and the contact stresses. This assumption is necessary due to the two-dimensional modelling.

The analyses were carried out for the rail profile UIC60, the rail steel 900A, static wheel forces of 100kN and a train velocity of 250km/h. Head checks and squats are distinguished by their different inclination angles.

The experimental crack growth examinations of cold worked rail steel show a pronounced orthotropy of the fracture mechanical properties. Contrary to the original assumption that crack growth examinations under pure shear crack tip loading enables the determination of the wanted properties, the cracks branched immediately. Therefore the original intention of finding a criterion for the change of crack growth direction on an experimental basis could not be realized. The wanted fracture mechanical crack growth properties of the cold worked rail steel were found out under a Mixed-Mode I+II crack

tip loading. It is remarkable that the direction of crack propagation was influenced strongly by the direction of cold working despite the initial Mode I loading of the notch. Therefore a Mixed-Mode situation at the crack tip was present.

The analyses were formed as a Monte Carlo simulation in which the crack growth properties were taken into account dependent on the crack depth achieved. From the scatter field of the simulated crack propagation curves the curve with a crack growth speed of 90% was assumed as representative. This representative crack growth curve was modified to derive a curve for the assessment of the developing RCF cracks. The two variants of the assessment have to be understood as alternatives. Because of the missing of practical experiences these two variants have to be confirmed or modified by future practical experiences.

An assessment diagram for transverse cracks originating nearly from the running surface is derived by means of the fracture mechanics. This diagram shows that the rail temperature plays an essential role.

The fracture mechanical analyses show that the critical crack depth of secondary failures in the neighbourhood of an initial failure lay in the same size as developed RCF cracks. To guarantee the safety of the railway service, none of the multiple RCF cracks should deviate in the transverse direction.

In future analyses the residual stresses of used rails and the real crack front geometry according the statistically analysed service failures should be included.

REFERENCES

[1] ERRI-Frage D 173 *„Ermüdung durch Rad-Schiene-Kontakt“: Spannungsanalyse der Ermüdungsrisse durch Rad-Schiene-Kontakt – Zwischenbericht (1988 – 1992)*. European Rail Research Institute (ERRI), Utrecht, ERRI-Bericht D 173 / RP 11, Juni 1995.

[2] L. A. Chellani: *Rail Defects*. Indian Railways Technical Bulletin **35** (1978), Nr. 205, Seite 61 – 73.

[3] ORE-Frage D 88: *Untersuchung der Schienenfehler im Gleis. Bericht Nr. 5 „Vereinheitlichte Statistiken über das Auswechseln von Schienen im Jahre 1965. Schienenbrüche, die zu Entgleisungen geführt haben.“* Forschungs- und Versuchsamt des Internationalen Eisenbahnverbandes, Utrecht, ORE-Bericht D 88 / RP 5, April 1968.

[4] …: *Train Derailment at Hatfield, 17 OCTOBER 2000*, Second HSE interim report, 23 January 2001.

[5] T. Schnitzer, K.-O. Edel, I. Bohne: *Fahrflächenschäden*. Abschlußbericht für die Klaproth-Stiftung, Fachhochschule Brandenburg, August 2004.

[6] T. Schnitzer: *Bruchmechanische Analyse des Wachstums von Rollkontaktermüdungsrissen in Eisenbahnschienen*. Dissertation, Technische Universität Berlin, 2005.

[7] K.-O. Edel, G. Boudnitski, T. Schnitzer: *Schienenfehler und ihre bruchmechanische Behandlung*. 33. Tagung des DVM-Arbeitskreises Bruchvorgänge, Paderborn, 20./21. Februar 2001, DVM-Bericht 233 „Anwendung der Bruch- und Schädigungsmechanik“, Seite 163 – 180.

[8] T. Schnitzer: *Bruchmechanische Analyse der Rißausbreitung durch Rollkontaktermüdung*. Internationales Symposium „Schienenfehler“, 16. und 17. November 2000, Brandenburg an der Havel, Tagungsbericht, Seite 18-1 bis 18-20.

[9] S. Nishida: *Morphologic Study of the Shinkansen Rail based on Fracture Mechanics*. In: H. Nisitani (editor): Topic in Engineering, vol. 16 „Computational and Experimental Fracture Mechanics – Developments in Japan“, Computational Mechanics Publications, Southampton UK and Boston USA, 1994, Seite 379 – 408.

[10] H.-D. Grohmann: Personal information.

[11] K.-O. Edel: *Die Festlegung zulässiger Rißgrößen für Schienen und Schienenschweißungen auf der Grundlage der probabilistischen Bruchmechanik*. Forschungs- und Versuchsamt des Internationalen Eisenbahnverbandes, Utrecht, Technisches Dokument DT 183 (E 162), Januar 1987.

[12] K. Mutsubara: *Welded Rail Joint Fractures and their Effect on 200 km/h Operation*. Japan Railway Engineering **5** (1964) 3, Seite 21 – 24.